

Applications of single-wavelength anomalous dispersion at high and atomic resolution. Corrigendum

**D. E. Brodersen,^{a*} E. de La Fortelle,^b C. Vornrhein,^b
G. Bricogne,^{b,c} J. Nyborg^a and M. Kjeldgaard^a**

^aDepartment of Molecular Biology, University of Aarhus, Gustav Wieds Vej 10c, DK-8000 Aarhus C, Denmark, ^bMRC-LMB, Hills Road, Cambridge CB2 2QH, England, and ^cLURE, Bâtiment 209D, 91405 Orsay CEDEX, France.

Correspondence e-mail: deb@mb.au.dk

In the paper by Brodersen *et al.* [(2000), *Acta Cryst.* **D56**, 431–441] errors were published in values in the last set of

fractional coordinates and in the molecular mass. The correct values are given in this article.

In the article by Brodersen *et al.* (2000) there is an error in the values for the last set of fractional coordinates. The last sentence of the second paragraph on p. 434 should read 'In a direct-methods run applying 256 phase permutations, the positions of the two Ho atoms were determined to be (0.0676, 0.1540, 0.1048) and (0.0200, 0.3433, 0.0856) in fractional coordinates of the unit cell'. The error occurred because of a misreading of the log file from *SHELXS*.

Also, on p. 432 the molecular mass is listed incorrectly as 22.1 kDa. This should be given as 22.7 kDa.

References

Brodersen, D. E., de La Fortelle, E., Vornrhein, C., Bricogne, G., Nyborg, J. & Kjeldgaard, M. (2000). *Acta Cryst.* **D56**, 431–441.

Applications of single-wavelength anomalous dispersion at high and atomic resolution

D. E. Brodersen,^a E. de La Fortelle,^b C. Vonrhein,^b G. Bricogne,^{b,c} J. Nyborg^a and M. Kjeldgaard^{a*}^aMacromolecular Crystallography, IMSB, Aarhus University, Gustav Wieds Vej 10c, DK-8000 Aarhus C, Denmark, ^bMRC-LMB, Hills Road, Cambridge CB2 2QH, England, and ^cLURE, Bâtiment 209D, 91405 Orsay CEDEX, France

Present address: INSEAD, Boulevard de Constance, F-77305 Fontainebleau CEDEX, France.

Correspondence e-mail: mok@imsb.au.dk

Received 27 September 1999

Accepted 17 January 2000

Two examples of the application of single-wavelength anomalous dispersion (AD) in macromolecular structure determination are described, both using the statistical phasing program *SHAPE*. For the holmium-substituted calcium-binding protein psoriasin (22.7 kDa), a set of accurate phases has been obtained to a resolution of 1.05 Å without recourse to an atomic model of the molecule. The accuracy of the phases resulted in an electron-density map of a quality comparable to σ_A -weighted $2F_o - F_o$ maps derived from the final model refined with *SHELX 7*. Comparison of the refined and AD electron-density maps showed significant discrepancies resulting from the iterative refinement in reciprocal space. Additionally, it is shown that the structure of psoriasin can be determined from native data extending to 2.0 Å alone by exploiting the minute anomalous signal from a bound zinc ion.

1. Introduction

In order to construct an atomic model of a macromolecule by means of crystallography, it is necessary to turn the measured intensities of X-rays diffracted from a crystal into an electron-density map of sufficient quality for interpretation. This involves estimation of the phase angles, which are unmeasurable in crystallography, and tracing of an approximate atomic model in the electron-density map that results from Fourier transformation. The model is subsequently improved in the refinement process by taking into account stereochemical information, as well as by minimizing the discrepancy between measured structure factors and structure factors calculated from the model.

A technique for overcoming the problem of estimating the phases and obtaining an initial electron-density map which was pioneered by Perutz and co-workers, the multiple isomorphous replacement (MIR) method, yields good independent phase information (Green *et al.*, 1954). However, the quality of the phases tends to deteriorate rapidly with resolution owing to lack of isomorphism between native and heavy-atom substituted crystals. Consequently, the initial electron-density map may contain gross errors that prevent its proper interpretation in terms of a model. Reciprocal-space refinement of an incomplete structure model has been shown to involve the risk of model bias that can be difficult to escape later in the refinement (Hodel *et al.*, 1992). Molecular replacement is another powerful method for determining macromolecular structures that uses phase information derived from a similar protein structure (Rossmann & Blow, 1962). However, here too the partial correctness of the initial

model has important consequences for the progress of the subsequent refinement.

A special physical effect, namely the absorption of γ -rays by atoms at certain energies, also known as 'anomalous dispersion', can be used to yield independent phase information (Laue, 1916; Coster *et al.*, 1933; Honl, 1933; Bijvoet, 1944). The 'anomalous' signal, which is manifested in differences between Friedel-related reflections (the so-called Bijvoet differences), is usually small and requires accurate data collection and processing. However, the power and energy tunability of modern synchrotron beamlines have had profound impact on its use in recent years, most notably in the context of the multiple-wavelength anomalous dispersion (MAD) method (Hendrickson, 1991).

The traditional use of initial electron-density maps as a first poor sketch of the structure in which an approximate and perhaps incomplete atomic model can be traced has recently been challenged on two fronts. On the experimental side, the data collected at modern synchrotron-radiation beamlines have become much more accurate and complete (Helliwell, 1992; Dauter *et al.*, 1997) thanks to phosphor imaging-plate systems and CCD detectors, and the average time of data acquisition has decreased. Moreover, the advent of cryogenic technology (Haas, 1998; for a review, see Rodgers, 1997) has enabled crystals to diffract significantly longer in a strong γ -ray beam with minimal radiation damage. Therefore, one can now collect complete and highly redundant data sets from a single crystal, which again results in precise measurement of both diffraction intensities and their standard deviations. Likewise, improvements have also been achieved with respect to the software used to process the diffraction data (twinowski, 1993, 1997; Leslie, 1993; Ugurath, 1997) and new maximum-likelihood-based heavy-atom refinement and phasing algorithms have made it possible to more efficiently take advantage of small signals (La Fortelle & Bricogne, 1997).

The outcome is that under suitable conditions the initial electron-density map can now carry at least as much information as the final atomic model after refinement or the electron-density map derived from it. Burling and coworkers have shown that an experimental electron-density map calculated from a multiple-wavelength experiment at 1.8 Å resolution can provide useful information about multiple conformers of protein side chains and the organization of water molecules at the protein-solvent interface (Burling *et al.*, 1996; Lead, 1997). However, several experiments indicate that in some cases the anomalous signal available at a single wavelength can suffice for calculation of phases and thus structure determination (Hendrickson *et al.*, 1985). By analogy to the multiple-wavelength counterpart MAD (Hendrickson, 1991), phasing based on the Bijvoet differences only has been named single-wavelength anomalous dispersion or SAD. In general, phase estimation in such cases results in an ambiguity similar to the single isomorphous derivative (SID) case. In the original work by Hendrickson & Teeter (1981) for the determination of the structure of crambin, the phase ambiguity was resolved by combining the bimodal phase distribution with a

Table 1
Data-collection statistics.

Bound metal(s)	Holmium	Calcium, inc
Space group	2 ₁ 2 ₁ 1	4 ₃ 2 ₁ 2
Resolution range (Å)	37.5–1.05	1.5–2.05
Wavelength (Å)	0.01	0.862
No. of observations	700858	14331
	(160426 unique)	(1071 unique)
Unit-cell parameters (Å)		
<i>a</i>	46.753	51.6
	61.602	51.6
<i>c</i>	62.750	116.03
Temperature (K)	100	100
Completeness (%)	7. (84.0)	8. (100.0)
Redundancy	1.8 (1.2)	7.0 (6.0)
<i>R</i> _{sym} (%)	3.3 (10.8)	11.3 (42.3)
σ	26.0 (4.7)	15. (5.0)

Friedel mates separate. Values in parentheses represent the outermost resolution shell (1.07–1.05 Å). Values in parentheses represent the outermost resolution shell (2.12–2.05 Å).

minimum weight calculated from the known positions of the anomalous scatterers. This approach has been used in the determination of several other crystal structures, including trimeric haemerythrin (Mith *et al.*, 1983) and gramicidin A (Callace, 1986; Callace *et al.*, 1990). Combination of direct methods and single-wavelength anomalous scattering, known as iterative single-wavelength anomalous scattering (ISAS)

(Ang, 1985) has been used to break the phase ambiguity for a number of structures including metallothionin (Furey *et al.*, 1986), bovine neurophysin II in complex with a dipeptide (Chen *et al.*, 1991), the N-terminal fragment of IF3 (Biou *et al.*, 1995) and rusticyanin (Harvey *et al.*, 1988).

Phasing protocols using single-wavelength data all require a strong anomalous signal from heavy atoms such as iodine (neurophysin II), lead (IF3N), caesium (gramicidin A) or cadmium (metallothionin) and generally lead to relatively good electron-density maps. In cases where only a weak signal is available, however, other techniques must be employed before tracing the chain, for example, molecular replacement (Coyer *et al.*, 1988), or data must be collected very close to the absorption edge of the anomalous scatterer (Harvey *et al.*, 1988). However, Dauter and coworkers have recently demonstrated that by mimicking Cu α radiation at a synchrotron source, the anomalous signal produced by a large number of Fe and Cl atoms in a lysozyme crystal can be used to solve the phase problem for data collected away from the absorption edge (Dauter *et al.*, 1998).

The work presented here shows two examples of the phase information that can be extracted from single-wavelength diffraction experiments in the case of a 22.1 kDa dimeric calcium-binding protein. When calcium is substituted by a strong anomalous scatterer, holmium, we show that diffraction data collected far from the absorption edge but to true atomic resolution can be used to calculate an initial electron-density map of outstanding quality. Comparison with the refined 2.0- σ -*c* map has revealed notable differences resulting from the iterative refinement of the structure in reciprocal space. This observation has implications for our understanding of model-bias phenomena at this level of resolution. In

Table 2
Analysis of the anomalous signal and phasing statistics.

Resolution bin (Å)	37.5–2.4	2.4–2.08	2.08–1.70	1.70–1.47	1.42–1.32	1.32–1.20	1.20–1.11	1.11–1.05	37.5–1.05
Number of reflections	4032	7172	176	103	11804	14068	1435	12461	84587
$\langle I \rangle$	374.5	217.1	128.6	81.6	57.	43.	34.3	26.1	86.0
$\langle \sigma(I) \rangle$	4.5	3.16	1.77	1.54	1.46	1.63	1.6	2.37	2.07
$\langle \Delta \rangle$	15.42	12.68	8.8	6.88	5.47	4.58	3.87	3.2	6.36
$\langle \sigma(\Delta) \rangle$	6.11	4.53	3.01	2.82	2.73	3.07	3.64	4.27	3.53
$\langle \Delta \rangle / \langle \sigma(\Delta) \rangle$	2.5	2.8	3.0	2.4	2.0	1.5	1.1	0.8	1.8
r.m.s. (Δ) / r.m.s. (I)	4.8	7.1	7.	.5	10.8	11.8	12.8	14.0	10.7
C (phasing)	5.6	73.5	82.7	86.1	86.0	84.1	81.8	80.0	81.4
C (dens.mod.)	84.0	2.	5.2	5.5	5.0	3.6	1.	88.0	2.6
$\Delta\varphi$ (phasing)†	43.0	32.2	27.1	25.8	26.0	28.8	32.4	34.3	30.24
$\Delta\varphi$ (dens.mod.)	32.0	18.7	15.1	13.0	13.8	16.5	1.5	26.4	18.44

Δ is the Bijvoet difference, which is defined as $\Delta = I_{hkl} - I_{\bar{h}\bar{k}\bar{l}}$. Calculated as $[(1/\sum_i \Delta_i^2)^{1/2} [(1/\sum_i I_i^2)^{1/2} - C]]$. C is the average correlation between the set of phases calculated from the final refined model (φ_c) and the phases output directly from *SHA* (phasing) and after density modification (dens.mod.). † $\Delta\varphi$ is the average non-weighted difference between phases calculated from the final refined model (φ_c) and the phases output directly from *SHA* (phasing) and after density modification (dens.mod.).

another experiment with weaker diffracting crystals of the native protein, we demonstrate that for data collected far from the absorption edge and without fine energy tuning, the faint anomalous signal produced by a single incision can be used to calculate a good electron-density map to a resolution of 2.0 Å. This shows that the structure of the protein and most likely other metal-binding proteins can be determined *a priori* from a single native data set at this resolution without the use of a known model, heavy atoms or direct methods.

The AD-phased electron-density maps are especially useful because they provide information that is independent of any assumption based on an atomic model of the protein. The maps rely on no parameters other than those introduced to carry out heavy-atom refinement. In addition, the solvent fraction in the crystal and the assumption that there is a boundary between protein atoms and solvent atoms were used in the solvent-attenuating step. The independence of the electron-density maps from model hypotheses used in refining the protein model makes it possible to check the validity of the model and thus help start refinement closer to the optimal structure and reduce the risk of model bias.

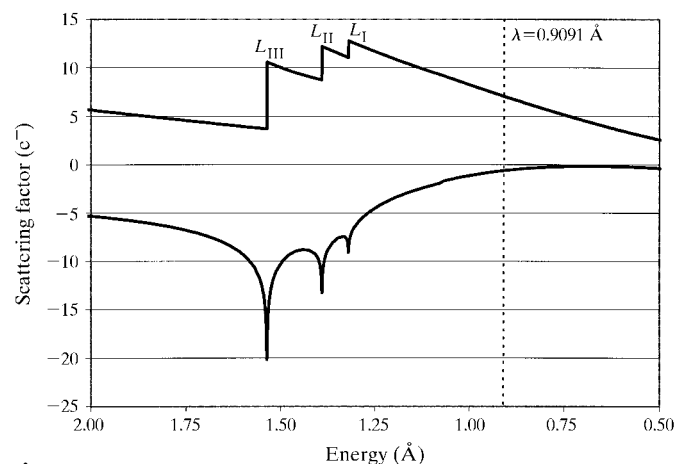


Figure 1
The three *L* absorption edges of the lanthanide holmium are located at 1.5362 (*L*_{III}), 1.303 (*L*_{II}) and 1.318 Å (*L*_I). The wavelength used for the AD experiment with holmium-substituted psoriasis, 0.9091 Å, is indicated with a vertical dashed line. At this point, the theoretical values of σ' and σ'' are -0.628 and $7.102 e^-$, respectively.

2. Methods

2.1. High-resolution AD experiment

2.1.1. Data collection. Monochromatic diffraction data were collected to a resolution of 1.05 Å at the 11 beamline, EMBL, Hamburg, Germany, for crystals of a holmium-substituted ($^{67}\text{Ho}^{3+}$) preparation of the 22.7 kDa dimeric calcium-binding 100 protein psoriasis (100A7) as previously reported (Brodersen *et al.*, 1998). In order to determine properly the intensities of the strongest reflections at this resolution, the data were collected in three consecutive runs (50–2.8 Å crystal-to-detector distance, 440 mm $\Delta\varphi = 2^\circ$; 15–1.7 Å crystal-to-detector distance, 250 mm $\Delta\varphi = 2^\circ$; 5.3–1.05 Å crystal-to-detector distance, 120 mm $\Delta\varphi = 0.5^\circ$). The crystals belong to the space group $P2_12_12_1$, with unit-cell parameters $a = 46.81$, $b = 61.63$, $c = 62.77$ Å, and diffract extremely well (1.0 Å). The data were reduced and processed using the *EMSCALE* AC suite of programs (twinowski & Minor, 1997; twinowski, 1993) and have an overall σ of 28.8 and an σ_{sym} of 4.3 (see Table 1 for data-collection statistics). Structure-factor amplitudes were calculated

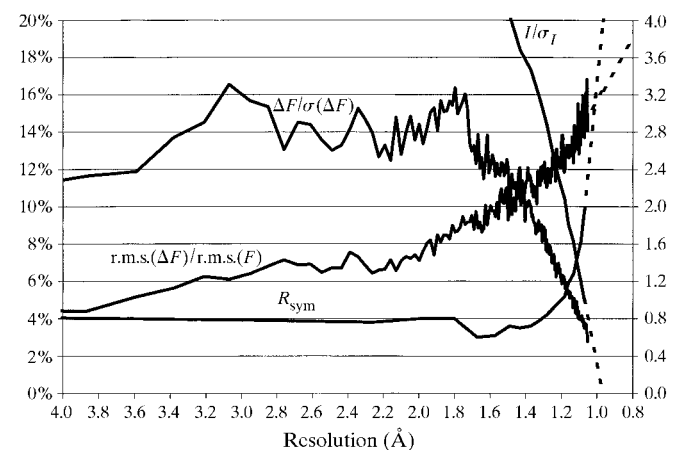


Figure 2
The breakdown with resolution of several crystallographic data quality indicators. The σ_{sym} and r.m.s. (Δ) / r.m.s. (I) are measured in percentages on the left y axis, whereas σ and $|\Delta| / \sigma(\Delta)$ are absolute numbers (right y axis). The r.m.s. (Δ) / r.m.s. (I) shows the average relative contribution of the anomalous signal in resolution bins and $|\Delta| / \sigma(\Delta)$ the signal-to-noise level of the anomalous differences.

Table 1. Refined heavy-atom parameters.

Ho1	0.331
<i>y</i>	0.3457
isocapacity	0.1048
Ho2	1.72
<i>y</i>	0.803
isocapacity	0.1565
scattering factors (e ⁻)	0.0860
'	0.6
"	-5.0
	6.7

Parameter was fixed during refinement in *SHA*.

using the *CC4* program (Collaborative Computational Project, Number 4, 1994; French & Wilson, 1978).

2.1.2. Heavy-atom detection and refinement. No special wavelength-stabilization apparatus was used because the data

were collected at a wavelength of 0.01 Å (13.6 keV), far from any of the holmium *L* absorption edges (*L*_I 1.31 Å, *L*_{II} 1.303 Å, *L*_{III} 1.5362 Å). The data were thus collected at the high-energy side of the *L*_I edge, where both μ' and μ'' are well tabulated and insensitive to small wavelength fluctuations. The fact that μ'' remains large in this range (~ 7.1 e⁻) gives rise to the significant anomalous differences shown in Tables 2 and 3.

From an anomalous difference Patterson, it was known that the monomers of this dimeric protein only contained a single holmium ion each, a total of two ions per asymmetric unit. This information, along with the Δs for unique reflections (37.5–1.05 Å) where both Friedel mates had been recorded, was input into the program *SHELXS* (Holdrick, 1981). In a direct-methods run applying 256 phase permutations, the positions of the two Ho atoms were determined to be (0.0676, 0.1540, 0.1048) and (0.200, 0.3433, 0.1548) in fractional coordinates of the unit cell.

2.1.3. Phasing. The positions and identities of the two heavy atoms along with the observed anomalous differences and structure factors were input to *SHA* (La Fortelle & Bricogne, 1977) in a heavy-atom parameter refinement and phasing run (see Table 3 for a summary of the refined heavy-atom parameters). The *SHA* phasing resulted in an overall figure of merit (FOM) of 82.6%. To further improve the quality of the initial map, the data were subjected to 70 cycles of solvent flattening using the program *SOLVENT* (Abrahams & Leslie, 1966; Collaborative Computational Project, Number 4, 1994) in a script implemented into the *SHA* interface in which the radius of the 'solvent sphere' is gradually reduced from an initial value of 5.0 Å to the maximum resolution of the data (1.05 Å in this case). This crystal form is tightly packed and contains approximately 40 solvent. Electron-density maps were calculated with *DMT* and *EXE* (Collaborative Computational Project, Number 4, 1994) and displayed in the program (Jones & Kjeldgaard, 1977). σ_A -weighted $2F_o - F_c$ maps representing the final refined map from the *SHELX* refinement were calculated using the *SHELX77* utility program *SHELXD*.

2.2. Direct phasing using native data

2.2.1. Data collection. Monochromatic γ -ray diffraction data were collected on a tetragonal crystal of the native protein to a resolution of 2.0 Å using an γ -ray wavelength of 0.863 Å (Table 1). Crystals of the native protein that appear in the presence of zinc belong to the space group *I*₄²₁², with unit-cell parameters *a* = 51.55, *c* = 116.033 Å (Nolsøe *et al.*, 1977; Brodersen *et al.*, 1998). This data set is 8% complete for all data between 1.0 and 2.05 Å. The data set was processed with the *EMSCALE* suite, taking into account the small but measurable anomalous signal

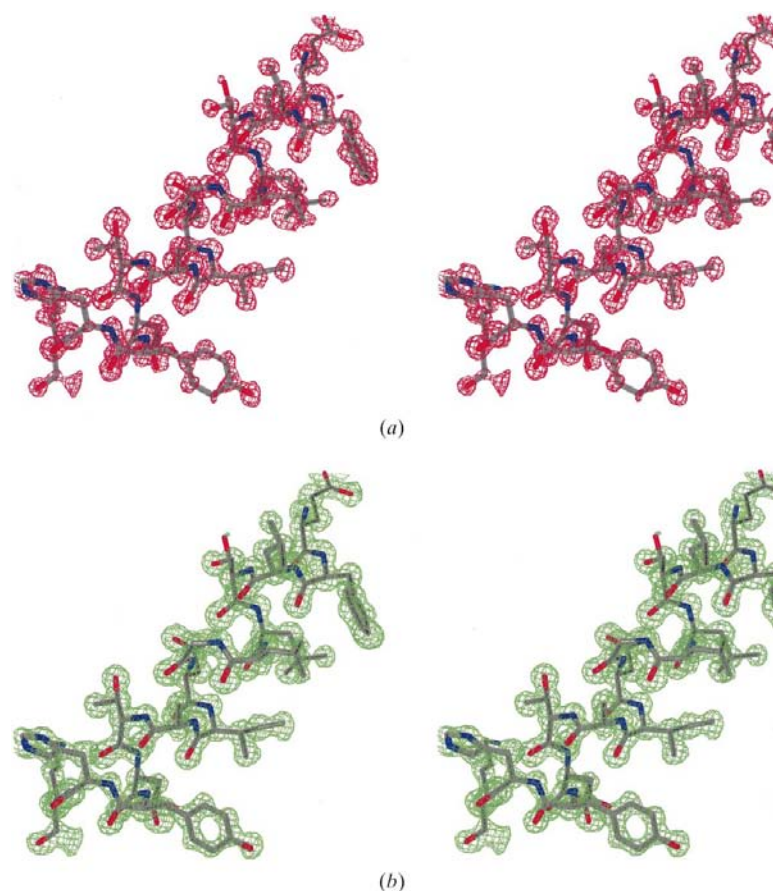


Figure 1. Two stereographs of the electron density resulting from the AD experiment with holmium-psoriasisin. (a) Map calculated with phases directly from *SHA*, i.e. without any kind of density modification. Contouring is 1.1 r.m.s. (1.11 e Å⁻³). (b) The final AD electron density after solvent flattening in *SOLVENT*. Contouring is 1.6 r.m.s. (0.3 e Å⁻³).

from the incident structure factors and anomalous differences were calculated using *CAFFE*. The orientation of the protein dimer within the unit cell was determined by molecular replacement using the previously determined structure of holmium-substituted psoriasin (Brodersen *et al.*, 1988) and the program *Amoeb* (Nava *et al.*, 1994). This showed that the protein crystallizes with a single monomer (100 residues) in the asymmetric unit, containing one bound calcium and one bound incident ion (Brodersen *et al.*, 1988).

2.2.2. Heavy-atom detection. The anomalous differences calculated with *CAFFE* were sorted based on the relative contribution of the observed structure factor. Only reflections for which $|\Delta| > 0.25$ were kept. When calculating the anomalous Patterson summation, the reflections were additionally subjected to an absolute value criterion in that only reflections which satisfied $|\Delta| > 50.0$ were used in the Patterson calculation. This resulted in 1577 reflections out of 11 213 (14%) being rejected.

2.2.3. Phasing. The single position of the incident ion was used along with the structure-factor magnitudes and anomalous differences to calculate optimal complete structure factors and phase distributions using *SHARP* (La Fortelle & Bricogne, 1997). In the density-modification step, 130 cycles of solvent flattening were carried out using *SHELXL* and the method of

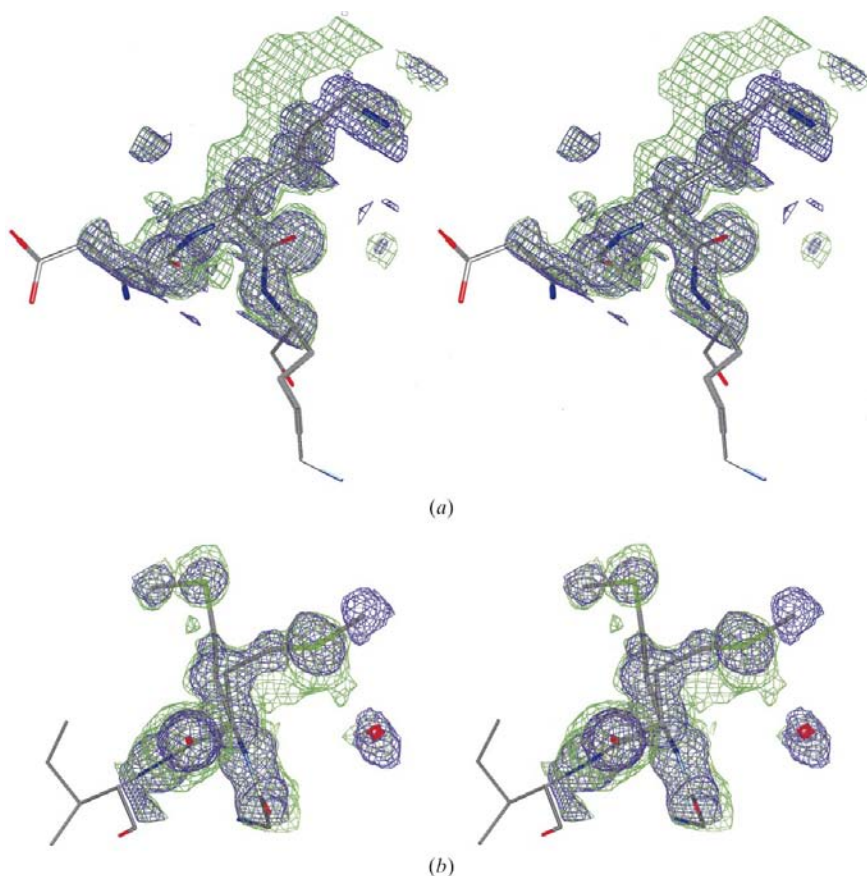
reducing the radius of the solvent sphere described above. The solvent radius was again reduced from an initial value of 5.0 Å down to the maximum resolution of the data, 2.0 Å. This crystal form contains approximately 60% solvent. Correlation coefficients were calculated with *AMoRE* (Kleywegt & Jones, 1996).

Results

1. High-resolution AD experiment

Single-wavelength anomalous diffraction (AD) data were collected to a resolution of 1.05 Å at a synchrotron source for a crystal of the holmium-substituted calcium-binding 100-protein psoriasin (100A7) at a wavelength of 0.01 Å (13.640 keV Brodersen *et al.*, 1988). For a data-collection summary, see Table 1. At this energy, the anomalous signal of the two Ho atoms bound to the dimeric protein is significant even though the wavelength is far from any of the *L* absorption edges of this lanthanide element (Fig. 1). Because of the very intense diffraction from these derivative crystals, the data set was collected in three consecutive runs corresponding to low, medium and high resolution (Table 1).

In cases where the temperature factors of the anomalous diffractors are much lower than the average temperature factor of the protein atoms, the expected anomalous signal represented by differences between Friedel reflections will increase with resolution on a relative scale. To estimate the measurable signal, the anomalous differences must then be compared with the measurement noise, which also increases with resolution. Fig. 2 shows the resolution dependence of the relative anomalous signal $\text{r.m.s.}(\Delta) / \text{r.m.s.}(\sigma)$ and the significance of the anomalous signal $|\Delta| / \sigma(\Delta)$, along with the crystallographic symmetry factor and σ for the measured intensities. Even for the highest resolution bin, the increased measurement noise does not bury the anomalous signal. In addition, the anomalous signal as measured by $|\Delta| / \sigma(\Delta)$ remains higher than 1.0 for all but the last bin (Table 2). In other words, the anomalous signal is significant to at least 1.1 Å resolution. $|\Delta| / \sigma(\Delta)$ for the whole resolution range is 1.8. In this case, the anomalous signal represents almost 15% of the intensities of the highest order reflections. Therefore, a systematic treatment of the Bijvoet differences at high resolution is of great value in the initial phase estimation. However, we believe that the overall data quality, rather than a high contribution, makes the anomalous signal a reliable source of information.



Figure

Two stereographs comparing the AD and refined electron density. (a) Residue LysA48 with refined 2- σ density from *SHELX* at 1.5 r.m.s. (0.26 e \AA^{-3} , blue) and AD density at 1.0 r.m.s. (0.617 e \AA^{-3} , green). (b) Residue MetA12 and a water molecule shown with the same maps as above.

2. heavy-atom detection and phasing

Since holmium had been introduced to replace the calcium ions which are naturally bound in the protein, detection of the holmium positions in the Patterson map was relatively straightforward owing to the existence of only two clearly defined and high-occupancy heavy-atom sites in the structure. Both heavy-atom positions could be found either by direct methods using the program *SHELXS* (Heldrick, 1983; Heldrick & Schneider, 1987), by manual interpretation of the anomalous Patterson function or from Patterson superposition methods (Heldrick, 1987).

Once the positions of the two Ho atoms in the asymmetric unit were located, parameters were refined and phasing was carried out using the statistical phasing program *SHA* (La Fortelle & Bricogne, 1987). The parameters representing the occupancies and the atomic scattering factors are strongly correlated in a MAD refinement. Therefore, the occupancy of the first heavy atom was fixed at 1.0 and the f' value for holmium fixed at an arbitrary value of $-5.0 e^-$, while f'' was refined along with the positional parameters, temperature factors and the occupancy for the other Ho atom. Table 3 shows the refined heavy-atom parameters. The imaginary part of the atomic scattering factor for holmium, f'' , refines to $6.7 e^-$, very close to the corresponding theoretical value of $7.1 e^-$.

The electron density could be further improved by use of solvent flattening as implemented in the program *S L* (Abrahams & Leslie, 1986; Collaborative Computational Project, Number 4, 1984). The procedure used, which gradually produces a finer mask, results in the determination of a final molecular envelope that closely fits the electron density of the molecule, including structural waters.

Well defined spherical solvent molecules are thus strengthened rather than attenuated. The map calculated from the solvent-attenuated phases will be referred to as the AD map in the following sections.

The overall correlation between phases calculated from the final model refined in *SHELX 7* and the phases output directly from *SHA* is 81.4%. Fig. 3(a) shows the electron density for one part of an α -helix of the protein, but the general quality of the map is similar even for regions outside stable secondary structure. In this map, which has not been subjected to any density modification, very fine details are visible such as atomic detail of the main chain and rigid aliphatic side chains, and static disorder (notice the multiple conformations of the serine residue in the lower left part of the figure). Table 2 shows the correlation between the phases output from *SHA* and phases calculated from the final refined model in resolution bins. Evidently, the correlation between the phase sets is highest between 1.7 and 1.3 Å and lowest below 2.0 Å, probably owing to poor modelling of bulk solvent in the refined structure.

After the density-modification step, the correlation between the two sets of phases is almost perfect (0.96). The highest resolution shell has a somewhat lower correlation, perhaps indicating that the molecular mask still needs refining. Fig. 3(b)

illustrates the final electron-density map calculated from the measured structure-factor magnitudes and the phases output from *S L*. The map shows clear atomicity and resembles to a large extent the final refined $2 - \sigma$ map from the refinement in *SHELX*.

Model bias

The model of the protein was originally traced in a map calculated from MAD phases extending to 1.0 Å, with the 1.05 Å data set being collected on a different crystal (Brodersen *et al.*, 1988). The high-resolution data set was then used for refinement of the model with the program *SHELX 7* (Heldrick, 1983; Heldrick & Schneider, 1987). The iterative least-squares refinement resulted in an overall crystallographic R factor of 10.4% for all data, with a cross-validation R_{free} value of 14.12% for a random 30% test set. The final refined model is used for all comparisons in this paper.

Owing to the atomic resolution data, the observation-to-parameter ratio, even with anisotropic factors, approaches that seen in small-molecule X-ray studies (160 437 observations (the Friedel mates being held separate) and 18 753 parameters, giving an overall ratio of 8.6). The traditional refinement included all the features expected at this level of resolution, such as riding H atoms, full anisotropic AD refinement and local static disorder. We believed initially that with the combination of a high observation-to-parameter ratio, excellent data quality, a well established high-resolution refinement protocol and very good refinement statistics, the model could not be improved upon at the end of refinement. However, as we will show in the following, the refinement protocol allowed some bias to remain in the final high-resolution model.

The phases resulting from the solvent-attenuation procedure described in the previous section are very accurate to the highest resolution. The AD map thus offers the unique possibility of studying important structural features of a macromolecule at atomic resolution. Although the AD map (Fig. 3) fits the refined model almost perfectly, it also provides additional information in its fine detail. By comparing the AD map with the final σ_A -weighted $2 - \sigma$ map from the *SHELX* refinement, we have been able to locate several occurrences of model bias either resulting from the iterative comparison of calculated and measured structure factors or from phase errors present when the initial MAD map was calculated. This shows that interpretation of the electron density as an atomic model *alays* affects the result, regardless of the degree of overdetermination of the set of parameters to be estimated (*i.e.* positional coordinates and temperature factors).

Improved modelling of multiple conformers

Static disorder is a common phenomenon and from high-resolution studies it is estimated that between 6 and 15% of all residues in a protein are likely to exist in more than one single conformation (Mith *et al.*, 1986). In this case, 10% out of a total of 200 residues in the asymmetric unit (~ 10) were initially

modelled with double conformations. A high degree of disorder is often a cause of trouble in cases of average to poor data, relatively weak initial phases or low resolution, because the occupancies of the multiple conformers are less than unity and the density thus appears considerably weaker than for an average rigid side chain. Moreover, multiple conformations are often modelled towards the end of the refinement process, at which point the density will be strongly biased by phases calculated from the model. Global quality indicators such as R_{free} are generally not sensitive enough to catch errors caused by such low-occupancy conformations. Independent phase information is thus indispensable when it comes to determining the number of discrete variations as well as their individual significance, since phases calculated from a model tend to distort the picture and favour the modelled conformation.

Fig. 4(a) shows an example of a lysine side chain (LysA48) in the structure of psoriasis which appears as a single discrete conformer in the refined σ_A -weighted $2F_o - F_c$ map from *SHELX* (blue) even though the terminal atoms C^γ , C^ϵ , N^ζ show some signs of flexibility as judged from the density. This is also reflected in the values of the equivalent isotropic displacement factors for this residue, which appears near the end of an α -helix. Whereas the main chain and the first part of the side chain (until C^γ) is relatively rigid ($B_{\text{iso}} = 15 \text{ \AA}^2$), flexibility increases drastically near the terminus of the side chain (B_{iso} of 32 \AA^2 for C^ϵ and 42 \AA^2 for N^ζ). When investigating the AD map (green density), it is evident that this apparent thermal mobility is caused by a distinct double conformation of most of this side chain. Not even a σ_A -weighted $2F_o - F_c$ difference density map (not shown) reveals the true identity of this second side-chain orientation. Modelling of this side chain as a double conformation and refining the structure again significantly reduced the isotropic displacement factors for both conformations (B_{iso} of 26 and 21 \AA^2 for the two C^ϵ atoms and 37 and 22 \AA^2 for the two N^ζ atoms).

Fig. 4(b) shows the final $2F_o - F_c$ electron density around a methionine residue (MetA12, blue) along with the same region of the AD map (green). This methionine residue occurs in at least two different orientations which are clearly identified from the two positions of the dense sulfur atom. However, when comparing the model with the AD density (green), it is obvious that the C^ϵ position for one of the conformations is incorrect. Modelling of the C^ϵ position as pointing upwards earlier in the refinement has resulted in artefactual density appearing in this position (blue density). The peak in the density at the real position of the C^ϵ (towards the right) was mistakenly modelled by a water molecule, which has then supposedly been pushed away by anti-bumping restraints. For neither of the cases mentioned here did the σ_A -weighted difference density (Fourier coefficients $2F_o - F_c$) calculated by *SHELX* reveal the true conformation of the side chain.

For more than 20 amino-acid side chains, discrepancies between the AD map and the refined map were found, thus involving more than 10% of the protein. Some of these cases involved residues where the refined electron density only

revealed one out of two or more possible side-chain conformations. For other residues, the side chain had initially been modelled in an incorrect conformation and the real orientation did not appear in the $2F_o - F_c$ map. Finally, for some of the residues in the psoriasis structure it was discovered in the comparison with the AD map that only the low-occupancy conformation had been modelled. These errors could have arisen from slight differences between the crystal used for the 1.5 \AA MAD phasing and that used for the 1.05 \AA

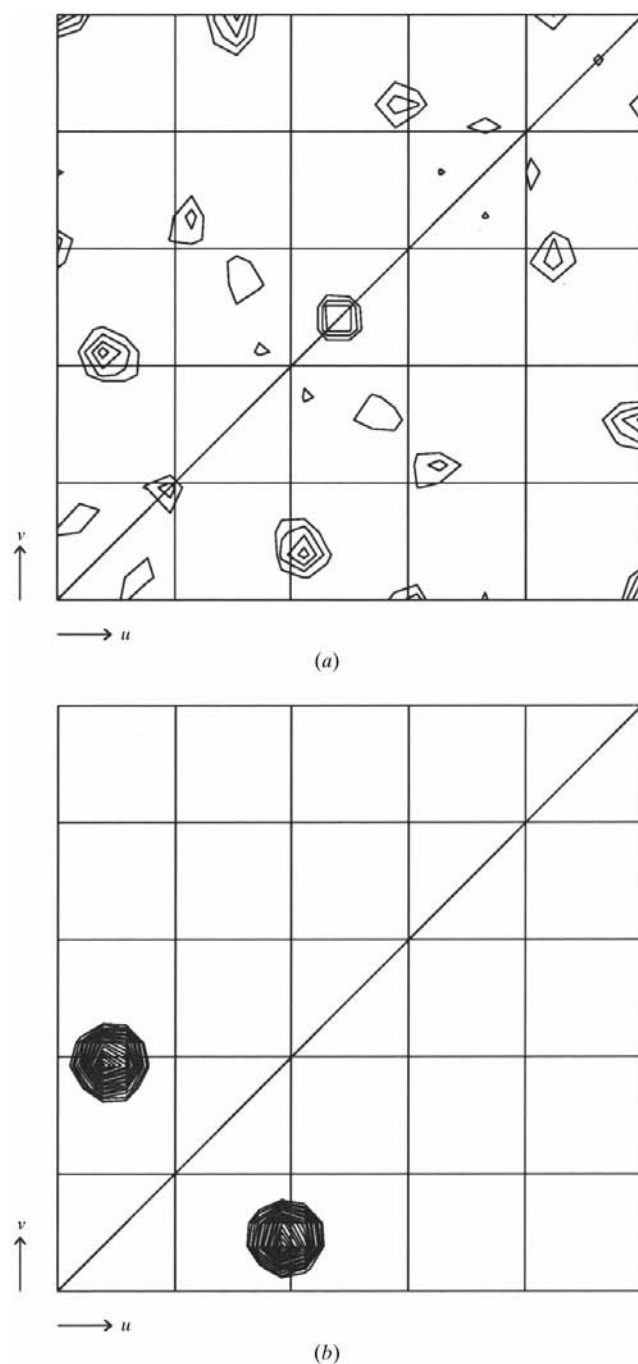


Figure
(a) The 14×14 Harker section of the filtered anomalous difference Patterson function. Contouring is 1σ to 10σ in 0.5σ steps. (b) The corresponding Patterson section calculated from the refined position of the sulfur atom.

refinement. They show, however, that even at atomic resolution, least-squares-based refinement cannot always escape the influence of the model-calculated phases.

Direct phasing using native data

The native calcium-bound psoriasis crystallises in two different space groups depending on whether divalent zinc is present or not and this has been shown to be the result of binding of zinc to a high-affinity site within the protein (Brodersen *et al.*, 1999). Crystals formed in the presence of zinc belong to the tetragonal space group $I4_32_12$ and diffract to about 2.0 Å. A native data set was originally collected at 0.863 Å (14.368 keV) from these crystals with molecular replacement in mind (for a data-collection summary see Table 1). The wavelength used for data collection is located on the high-energy side of the zinc absorption edge at 1.2837 Å (0.9660 keV), but far from the edge, at a point where the value of f'' is only 2.0 e⁻ or only about half of what would be observed close to the absorption edge.

Even though the structure was solved by molecular replacement, we have taken a thorough look at the anomalous Patterson function to see whether the position of the zinc atom within the unit cell can be found without the use of an initial search model. On average, the anomalous signal strength as measured by $|\Delta f|/\sigma(\Delta f)$ is less than one and the anomalous differences are only clearly significant below 3 Å resolution.

At higher resolution (even though the anomalous contribution theoretically should increase relative to f'') the anomalous signal is buried in measurement noise.

Given that the determination of heavy-atom positions by inspection of the Patterson function is one of the bottlenecks in phasing methods based on difference data [MI (A) MAD AD], the question is how to obtain the most from the available information. In this case, careful rejection of outliers turned out to be critical for interpretation of the anomalous Patterson function. Fig. 5(a) shows the Harker section 1/4 of the anomalous Patterson function calculated using all anomalous differences not exceeding 25% of the value of the observed structure factor. This is a very reasonable criterion, in that the signal even for the strongest anomalous scatterers at the absorption edge rarely constitutes more than 25% of the structure-factor amplitude. In addition to this relative magnitude criterion, a limit on the absolute $|\Delta f|$ was applied. The result of the filtering of the anomalous differences is a significant improvement in the signal-to-noise ratio of the relevant Harker section. In fact, the position of the zinc ion could not be determined from the non-filtered Patterson function (not shown). The correct peaks for determination of the coordinates of the zinc are now seen at about 2σ above the noise as the only peaks not on any axis. Fig. 5(b) shows the corresponding Patterson calculated from the zinc position.

The position of the single zinc ion in the asymmetric unit was now used for calculation of phase probability distributions in *SHAPE*. The resulting electron-density map is now of relatively poor quality and does not contain enough information for tracing of an initial model. The overall map correlation between the *SHAPE* map and the final refined 2- σ map is 22%. However, when subjected to 70 cycles of solvent flattening in *SHELX*, the map improves dramatically and the resulting electron density is of a quality close to the final refined map (Fig. 6). The overall map correlation between the solvent-flattened map and the final refined map is about 80%. In the solvent-flattened map, all parts of the protein main and side chains are visible and in some places multiple conformations can be seen.

6. Effect of completeness and redundancy

The data set used here is 90% complete and has a high redundancy of 7.0. In order to investigate the effect of these two parameters on the phasing, a series of truncated data sets were produced by gradually removing images at the end of the φ -range. In contrast to, for example, applying an upper resolution limit, this does not produce artificially truncated data since it merely corresponds to terminating the data collection at an earlier stage. As can be seen in Fig. 7, in such a case the redundancy will decrease almost linearly when images are removed, whereas the completeness will remain at almost 100% until a certain point where it starts to

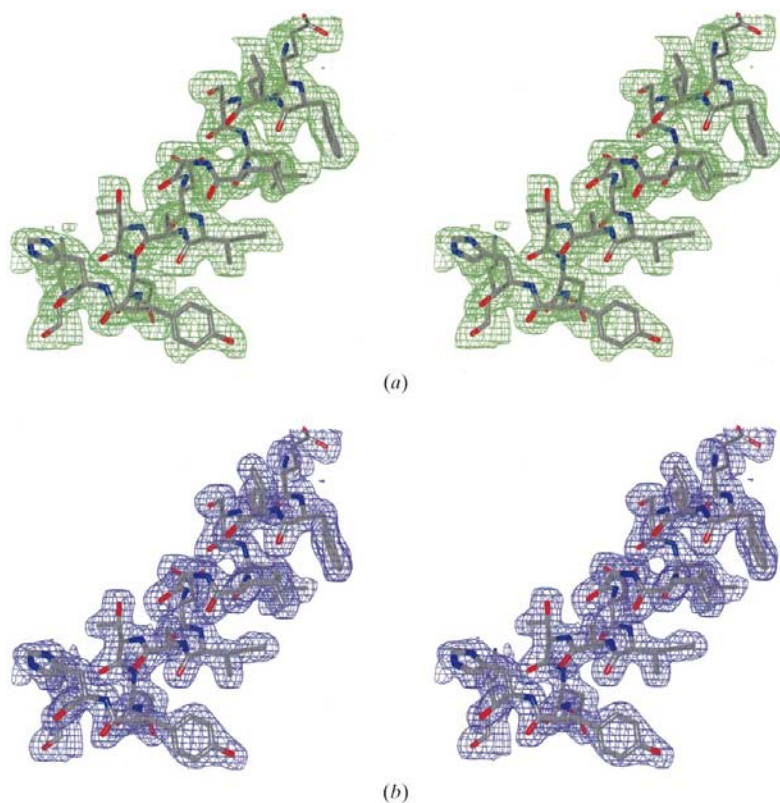


Figure 6

Two stereographs showing the electron density resulting from phasing with a single zinc ion. (a) The electron density after solvent flattening in *SHELX*. Contours are at 0.5σ . (b) The refined 2- σ electron density from *SHELX*. Contours are at 1.5σ .

drop dramatically. Phasing in *SHA* was carried out with 13 different truncated data sets ranging from the above 100 completeness and a redundancy of 7.0 down to 70 completeness and a redundancy of 1.5 (Fig. 7). As judged by the quality of the resulting electron-density maps, the outcome of the phasing does not seem to depend much on redundancy. At 8.7 completeness and a redundancy of 3.8, the correlation between the solvent-attenuated *SHA* map and the final refined map is still 72%. However, when the (anomalous) completeness starts to drop, the map correlation coefficients also deteriorate rapidly. In fact, at 3.3 completeness and a redundancy of 2.5, solvent attenuating is no longer able to bootstrap the initial phases. In other words, the final correlation reaches its maximum of 80% exactly at the point where the completeness reaches 100%. Thus, for reliable and consistent phasing using weak single-wavelength data, complete but not necessarily highly redundant data seems to be needed, provided it is measured accurately.

Discussion

In the experiment with AD phasing using the strong anomalous scatterer holmium, we compared the AD and $2 - c$ maps for our assessment of the extent of model bias. In a further step, however, we took advantage of the accuracy of the independent phases to calculate an unusual type of difference map with Fourier coefficients $(F_o - c, \varphi)$, where F_o represents the measured structure factors, F_c the structure factors calculated from the final model and φ the phases output from the solvent-attenuating step. This map shows a vast amount of detail close to the structure as well as long stretches of density in the solvent regions. Undoubtedly, this type of map presents valuable information with respect to

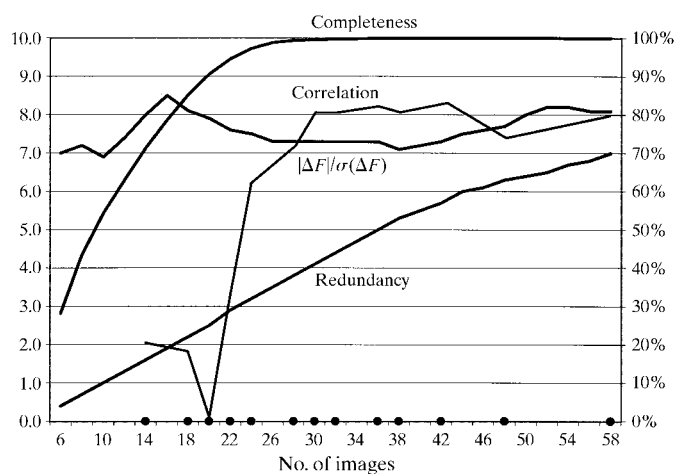


Figure
The breakdown of data completeness, redundancy and $|\Delta F|/\sigma(\Delta F)$ with the number of images included in the processing. 'Correlation' is the map correlation between the solvent-attenuated AD map output from *SHELX* at any given stage and the final refined $2 - c$ map from *SHELX*. Completeness, map correlation and $|\Delta F|/\sigma(\Delta F)$ are measured in percentage on the right y axis, whereas the redundancy is measured in absolute values on the left y axis. The solid circles on the x axis indicate the truncated data sets used for phasing.

the lack of ability of the refined model to describe the measured data. We did not, however, further assess the significance of this additional information, but this type of map could be valuable as an investigation tool in future studies.

Observing chemically reasonable density features in the AD map or in the AD-phased difference map is not sufficient by itself to justify an update of the model. After modelling of the additional conformers found from inspection of the AD map, the traditional cross-validation indicator (R_{free}) should theoretically decrease as a result of bias reduction. In these experiments, we have used the same 3-free set of reflections that was used in the original refinement against the 1.05 Å data to judge whether the side-chain modifications were significant. However, after a few more cycles of refinement in *SHELX 7*, we could not observe a significant change in R_{free} regardless of the resolution range. This is consistent with the idea that a global quality indicator based on a subset of the available measurements is insensitive to small alterations in the model. After all, the newly introduced conformations constitute few atoms all with occupancies well below unity and the total additional scattering power of these atoms is thus very small. In addition, it must be borne in mind that the same number of additional parameters are introduced to the refinement regardless of the occupancy of the atoms involved.

In another approach to assess the significance of the improved modelling, we used the same refinement program to estimate the standard deviations of the refined occupancies of the additional side-chain conformations. Inversion of the full least-squares matrix for all but the smallest proteins is a computationally challenging procedure. However, by fixing the positional parameters of all atoms we were able to invert the full Hessian matrix consisting of atomic displacement parameters and occupancies for the entire protein (200 residues). For the lysine residue mentioned above (LysA48), the occupancies of the two conformations refine to 0.771 (old conformation) and 0.22 (new conformation) with an estimated standard deviation (e.s.d.) of 0.018. The reason there is only one e.s.d. per two conformations is that modelling of a double conformation only introduces one additional parameter, namely the occupancy of the first conformation α . The occupancy of the second conformation is then constrained to $1 - \alpha$. The overall results show that all additional conformations are indeed significant at the 3σ level.

The apparent contradiction between the R_{free} and the e.s.d.s can be explained by the lack of sensitivity of the free factor as a significance test in this case. Most of the information concerning the alternate conformations resides in the high-resolution data and a 3-sample may not be enough for proper cross-validation of these fine details. This lack of sensitivity could also arise from an inherent inability of the atomic parameter model to represent accurately high-resolution features in the electron density. While an atomic model provides a convenient way to exchange information about a molecule (or store it in a database), it may only be one of several possible interpretations of the experimental data. Thus, to represent certain features of a structural model, an

electron-density map calculated from good phase estimates can in some cases provide more information than the refined atomic model. However, when the phases are relatively weak, describing the phases by discrete phase values (as required to perform a Fourier transform) is not a satisfactory approximation. In such cases, the resulting phase probability distribution is broader and possibly bimodal, which makes it impossible to approximate by a single phase value.

When the phase information is too weak to provide an accurate initial electron-density map, the experimental information is best represented in reciprocal space as structure-factor amplitudes with phase probability distributions. To use this information with the least possible bias, it is necessary to refine the atomic model against a maximum-likelihood target in reciprocal space. This approach has recently been implemented in several programs (X-PLOR, Brunger *et al.*, 1987; E-AC, Murshudov *et al.*, 1997; SHELX, Bricogne, 1993, 1997; Bricogne & Irwin, 1996) however, none of these programs yet support both refinement of anisotropic factors and partially occupied conformations.

The quality of the phase estimates which are based on the single-wavelength anomalous signal from zinc is remarkable for data at this resolution (2.0 Å). Compared with a structure solution by molecular replacement alone, this approach produces an electron-density map free from bias of any search model, as only the position of the zinc atom is used for phasing.

Our results do not only prove the usefulness of density-modification procedures in phasing, but also the power of SHAPE to create a precise initial envelope of the molecule. In other words, the map correlation coefficient calculated directly after the SHAPE run is not a good indicator of the quality of the calculated phases. The real discriminator is the density-modification procedure, which is capable of dramatically improving the map quality in the case of a useful initial envelope.

Conclusions

The present study first of all underlines the fact that anomalous scattering, when present, provides extremely valuable phase information to high resolution. In addition, AD phasing has an important and usually overlooked advantage over I phasing. In AD, the knowledge of the heavy-atom substructure can be used not only to model the anomalous diffraction but also to predict the normal diffraction of these atoms as a known fragment of the whole molecule. Taking this information into account (which is automatically performed in SHAPE) significantly reduces the degree of bimodality in the phase probability distribution as described by Hendrickson & Teeter (1981).

In practice, any detectable anomalous signal should be exploited even if the data was not deliberately collected to optimize it. In general, it is likely that AD phasing can be carried out as far as the resolution limit for crystals containing anomalous scatterers. Such scatterers are either naturally present in the macromolecule or can be introduced by a number of well known techniques (e-Met, heavy-atom

derivatives, bromouridine *etc.*). Even zinc atoms have been shown to be useful sources of anomalous signal in some cases (Hendrickson & Teeter, 1981; Dauter *et al.*, 1998). Phases derived from such experiments will not only help to reduce bias in crystallographic refinement, but also in structure solution by molecular replacement as well as ligand-binding studies using Fourier difference maps.

The results presented in this paper also demonstrate the importance of proper data treatment in macromolecular crystallography. Significant anomalous or isomorphous differences may be partly disguised by badly measured intensities and can thus impede the direct determination of heavy-atom positions. Additionally, we have shown that near-complete (anomalous) data is crucial for the estimation of initial phases by the AD method. In the case of molecular replacement, a small anomalous signal can help circumvent model bias. Our results also show that with modern phasing techniques based on fully phased maximum likelihood (such as SHAPE in combination with SHELX), less information is required to produce an interpretable map than has been the case previously. Here, we have shown how an ordinary 2.0 Å native data set, which was not even collected to maximize the anomalous contribution of the zinc, can be used to solve the structure of human psoriasis from scratch. Thus, for relatively small metal-binding proteins, a full-blown multiple-wavelength (MAD) or multiple-derivative (MIR) experiment will in many cases be unnecessary.

The authors wish to thank Jørgen Nolsøe for collecting the original diffraction data on the calcium-bound psoriasis crystals and Dr Raymond Brown for help and discussions with respect to the filtering of anomalous differences. Funding was provided by a special programme for biotechnology under the Danish Natural Science Research Council and a Hallas-Møller fellowship from the Novo Nordisk Foundation to MK.

References

- Abrahams, J. P. & Leslie, A. G. W. (1986). *Acta Cryst.* **D5**, 30–42.
- Bijvoet, J. M. (1942). *Acta Cryst.* **A1**, 888–891.
- Biou, V., Chu, F. & Ramakrishnan, V. (1995). *Eur. J. Biochem.* **230**, 4056–4064.
- Bricogne, G. (1993). *Acta Cryst.* **D**, 37–60.
- Bricogne, G. (1997). *Acta Cryst.* **A53**, 14–19.
- Bricogne, G. & Irwin, J. J. (1996). *Crystallography in Molecular Biology*, edited by E. Dodson, M. Moore, A. Drenth & J. Bailey, pp. 85–122. Dordrecht: Daresbury Laboratory.
- Brodersen, D. E., Ederodt, M., Madsen, J., Thøgersen, H. C., Celis, J. E., Nyborg, J. & Kjeldgaard, M. (1998). *Structure*, **6**, 477–483.
- Brodersen, D. E., Nyborg, J. & Kjeldgaard, M. (1997). *Structure*, **5**, 165–170.
- Brunger, A. T., Kuriyan, J. & Karplus, M. (1987). *Science*, **235**, 458–460.
- Burling, F. T., Wilson, I., Flaherty, K. M. & Brunger, A. T. (1996). *Science*, **272**, 72–77.
- Chen, L., Drenth, J., Breslow, E., Wang, D., Chang, C.-C., Furey, J. F. Jr, Wang, M. & Wang, B.-C. (1991). *Proc. Natl. Acad. Sci. USA*, **88**, 4240–4244.
- Collaborative Computational Project, Number 4 (1994). *Acta Cryst.* **D5**, 760–763.

- Coster, D., Knol, K. & Rins, J. A. (1933). *J. Cryst. Growth*, **6**, 345–36.
- Dauter, S., Dauter, M., La Fortelle, E. de, Bricogne, G. & Heldrick, G. M. (1997). *J. Cryst. Growth*, **183**, 1–2.
- Dauter, S., Lamzin, V. & Wilson, K. (1997). *Cryst. Growth*, **183**, 681–688.
- French, G. & Wilson, K. (1978). *Acta Cryst. A*, **34**, 517–525.
- Furey, J. F., Robbins, A. H., Clancy, D., Ingle, B. C. & Stout, C. D. (1986). *Science*, **232**, 704–710.
- Green, D., Ingram, V. M. & Gerretsen, M. F. (1954). *Proc. Ser. A*, **5**, 287–307.
- Haas, D. J. (1968). *Acta Cryst. B*, **24**, 604.
- Harvey, I., Hao, Z., Duke, E. M. H., Inglede, J. & Hasnain, S. E. (1988). *Acta Cryst. D5*, **14**, 62–635.
- Helliwell, J. (1992). *Academic Lectures in Crystallography*. Cambridge University Press.
- Hendrickson, J. A. (1991). *Science*, **251**, 51–58.
- Hendrickson, J. A., Mith, J. L. & Heriff, J. (1985). *Acta Cryst. E*, **11**, 41–55.
- Hendrickson, J. A. & Teeter, M. M. (1981). *Acta Cryst. L*, **7**, 107–113.
- Hodel, A., Kim, S. & Brunger, A. T. (1992). *Acta Cryst. A*, **48**, 851–858.
- Honl, H. (1933). *J. Cryst. Growth*, **1**, 1–16.
- Jones, T. A. & Kjeldgaard, M. (1977). *Acta Cryst. E*, **3**, 173–207.
- Kleywegt, G. A. & Jones, T. A. (1996). *Acta Cryst. D5*, **22**, 826–828.
- La Fortelle, E. de & Bricogne, G. (1977). *Acta Cryst. E*, **3**, 472–474.
- Laue, M. von (1916). *Ann. Phys.*, **5**, 433–446.
- Leslie, A. (1993). *International Tables for Crystallography*, edited by L. Sawyer, N. Isaacs & S. Bailey, pp. 44–51. Daresbury Laboratory.
- Murshudov, G. N., Vagin, A. A. & Dodson, E. J. (1997). *Acta Cryst. D5*, **23**, 240–255.
- Nava, J. (1990). *Acta Cryst. A*, **46**, 61–620.
- Nava, J. (1994). *Acta Cryst. A5*, **20**, 157–163.
- Nolske, S., Thirup, S., Ederodt, M., Thøgersen, H. C. & Nyborg, J. (1997). *Acta Cryst. D5*, **23**, 11–121.
- twinnowski, J. (1993). *International Tables for Crystallography*, edited by L. Sawyer, N. Isaacs & S. Bailey, pp. 56–62. Daresbury Laboratory.
- twinnowski, J. & Minor, W. (1997). *Acta Cryst. E*, **23**, 307–326.
- Ugrath, J. (1997). *Acta Cryst. E*, **23**, 286–306.
- Upton, J. (1997). *Acta Cryst. E*, **23**, 11–14.
- Ward, D. (1997). *Acta Cryst. E*, **23**, 183–203.
- Wossmann, M. G. & Blow, D. M. (1962). *Acta Cryst.*, **18**, 24–31.
- Woyner, J. E. Jr, Hendrickson, J. A. & Chiancone, E. (1988). *Acta Cryst. E*, **14**, 21052–21061.
- heldrick, G. M. (1993). *SHELX 3: A Powerful Crystal Structure Refinement Program*. University of Göttingen, Germany.
- heldrick, G. M. (1997). *International Tables for Crystallography*, edited by S. Fortier, pp. 11–130. Dordrecht: Kluwer Academic Publishers.
- heldrick, G. M. & Schneider, T. (1997). *Acta Cryst. E*, **23**, 31–343.
- Mith, J. L., Hendrickson, J. A. & Addison, A. (1983). *Acta Cryst. L*, **9**, 86–88.
- Mith, J. L., Hendrickson, J. A., Honatko, B. & Heriff, J. (1996). *Acta Cryst. E*, **22**, 5018–5027.
- allace, B. A. (1986). *Acta Cryst. E*, **12**, 25–306.
- allace, B. A., Hendrickson, J. A. & Ravikumar, K. (1990). *Acta Cryst. B*, **16**, 440–446.
- ang, B.-C. (1985). *Acta Cryst. E*, **11**, 0–112.